International Journal of Technology

http://ijtech.eng.ui.ac.id

Research Article

Flexible Converter for Electric Vehicle Charging Station Using Renewable Energy Efficiently

Nguyen The Vinh [1,2,*], Nguyen Van Dung [3]

[1]Automation and Robotics Laboratory-ARL Lab, Posts and Telecommunications Institute of Technology Hanoi, Hanoi 12100, Vietnam
[2]Faculty of Electronic Engineering I, Posts and Telecommunications Institute of Technology Hanoi, Hanoi 12100, Vietnam
[3]School of Electrical and Electronic Engineering, Hanoi University of Industry, Hanoi City, Hanoi 11900, Vietnam
[*]Corresponding author: vinhnt@ptit.edu.vn; Tel.: +084 912224112

Abstract: This article presents the research content of a solution for DC/AC, DC/DC, and isolated AC/DC converters using three-winding pulse transformers to work flexibly with coils that can be primary and secondary. The ratio between the pairs of coils is calculated differently to suit the output voltage requirements for battery charging for EVs and AC microgrid loads with different voltage levels and frequencies. The number of turns of the coil connected to the EV charging station will be 10 times larger than the coils at other outlets, and the coil operates in either primary or secondary mode in the transformer. In this pulse transformer, components such as renewable energy sources of solar panels (PV) DC voltage output, distributed sources, loads, and storage systems in the AC microgrid capable of bidirectional conversion and connecting to the main grid are connected. The main load is the batteries of electric vehicles (EV) supplied with energy in DC from PV sources and from the AC microgrid at the same time or in each case from different energy sources. The converter performs stable and flexible scenario operation to help the EV charging system use renewable energy efficiently, increase the continuous supply of electricity to the AC microgrid load, help save electricity, and stabilize the power system. Simulation results using Orcad software describe the values of current, voltage can reach 1000 VDC for the EV charging station, average conversion power of nearly 10 kW, and the average efficiency achieved by the converter of nearly 96% compared with reference documents and experiments to draw initial conclusions for the research project.

Keywords: DC/DC Converter; DC/AC Converter; Electric car batteries; Inverter; Pulse transformer

1. Introduction

In fact, the growth and development of the electric vehicle market worldwide (Busch et al., 2024; Jones et al., 2023; Bukhariv et al., 2015; Young et al., 2013), as well as in Vietnam, is increasingly strong, becoming an inevitable trend for green life and green transportation (Ajiwiguna and Kirom, 2024; Balagopal et al., 2017; Fontaras et al., 2017). However, using electricity from traditional power plants, such as coal and gas thermal power plants, to supply EV charging stations is essentially still using fossil fuels, which cannot fully meet the goals of the Action Program on green energy transition, reducing carbon and methane emissions in the transportation sector (Decision No. 876) (Government of Vietnam, 2022).

Although there are many renewable energy sources in Vietnam, the main source of electricity for production and daily life is still lacking locally (Linh et al., 2024). With the rapid growth in the number of EVs today, the amount of new electricity consumed each year will increase significantly.

https://doi.org/10.14716/ijtech.v16i5.7701
Received March 2025; Revised May 2025; Accepted August 2025

It is necessary to have a solution to maximize the use of renewable energy resources to serve the charging of EVs to contribute to solving the abovementioned problem.

The converter for the charging system is developed with solutions suitable for the number and features of EVs (Islam et al., 2022; Khan et al., 2020; Chakraborty et al., 2019; Jayakumar et al., 2017; Hadley and Tsvetkova., 2009; Thomas et al., 2009; Bradley et al., 2009). Normally, on highways, roads far from residential areas have limited grid power. Al Sakka et al. (2011) reported that the IBC has an efficiency of 92% at a load of 30 kW. The efficiency drops by approximately 8% due to the conversion from discontinuous current mode (DCM) to continuous current mode (CCM). This converter is sensitive to changes in the duty cycle ratio. Furthermore, the influence of the magnetic core due to load changes is noticeable, and the number of components is high (Narasipuram and Mopidevi, 2023; Huangfu et al., 2021; Musavi et al., 2014; Hegazy et al., 2013).

In Vietnam, the development of electric vehicle charging station infrastructure is a decisive factor in the popularization and development of electric vehicles with the goal of making EVs the main means of transport in the future. The development of charging stations with superior features, integrating artificial intelligence (AI) with renewable energy, suitable for EVs using both alternating current (AC) and direct current (DC) power sources, compatible with both IOS and Android operating systems with remote control, fast and convenient payment has been and is actively contributing to this process, not only promoting the EV industry but also improving charging station infrastructure and using green energy, contributing to the construction of smart grids and sustainable urban areas in Vietnam (Government of Vietnam, 2018).

In Figure 1, the flexible converter is connected to three isolated ports by a transformer with three directly connected windings, namely, the renewable energy source (solar battery), the distributed AC grid, and the EV charging port. In this system, there is an independent renewable energy source that can be connected to supply electric energy to the EV charging station or to the AC microgrid. The distributed energy source from the AC microgrid is allowed to supply to the EV charging station. Thus, the EV charging station can receive electric energy from many supply ports with different power sources, such as AC or DC. The converter is derived from the basic converter such as fly-back DC/DC, the operating needs of the AC microgrid integrated with the renewable energy source (distributed energy source) flexibly and continuously supply energy. The advantage of isolated power transmission between ports ensures safety for independent ports. The flexible converters are derived from solutions from the documents presented by the author (Vinh and Dung, 2025; Vinh, 2023; Vinh et al., 2022; Thang et al., 2020). Centralized converters implement flexible energy conversion combining direct and isolated energy transfer by bidirectional converters connected to DC and AC microgrid systems integrated with renewable energy sources.

The charging speed depends on the AC, DC charger, and EV. Since not all AC and DC chargers and the converter on-board chargers have the same capacity, the AC and DC chargers must communicate with the EV to determine the required power and input current and establish a control connection to monitor the current during charging from the start to the end of charging (Jamahori, 2024; Onibonoje et al., 2023; Aravindan et al., 2023; Nurulin et al., 2023). This type of communication is called pilot wire communication. The pilot wire determines the type of charger attached to the EV so that the control can set the current to match the capacity of the charging AC or DC charger.

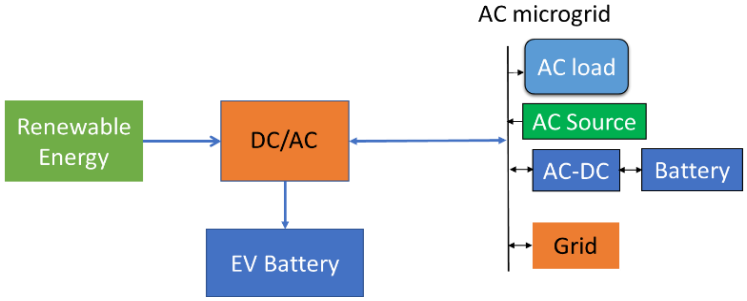

Figure 1 System structure diagram connecting the DC and AC microgrids

These types of batteries are the most dependable and prevailing innovation in the field of batteries for BEVs. The development of LIBs has been expanding in the last few years. Maximum BEVs in the future will be outfitted with LIBs. Examples of vehicles that use such types of batteries are the Tesla Roadster and the Mitsubishi i-Miev. These batteries are really reasonable for superior EV batteries because of the principle characteristics of this metal which is highly expected potential. This means that they have high potential energy (in Wh/kg). Among all the accessible metallic materials, lithium is additionally lighting weight. The lithium-ion battery's energy ranges from 60 to 250 Wh/kg, and its force capacity can be as high as 2000 W/kg (Rangarajan et al., 2022; Spingler et al., 2018; Wood et al., 2018; Yamamoto et al., 2014).

The nickel metal hydride (NiMH) battery is considered an advanced version of the nickel–cadmium battery due to the use of hydrogen inserted in metallic alloys instead of cadmium at the negative electrode. The NiMH battery is constantly sealed to prevent hydrogen leakage. It replaces nickel cadmium in the application of EVs due to the significant improvement in energy density of the nickel metal hydride battery. The utilization of nickel metal hydride batteries did not get commercialized in the 1990s because newer battery technologies were introduced very soon after the nickel metal hydride was developed (Liu et al., 2019; Ikeya et al., 2002).

The charging level of EVs is divided into 3 levels (Kopacz et al., 2024; Ahmad and Bilal, 2023; Dutta et al., 2022; Al-Ogaili et al., 2017) based on speed and capacity. Levels 1, 2, and 3 are three general terms that refer to the charging speed of EVs. Think of charging an EV as filling a swimming pool. Recharging an EV is similar to filling in a swimming pool, which can take minutes, hours, or days. It depends on the battery capacity of the car, the EVSE or charging station, and the on-board charger (OBC). In other words, charging an EV is similar to understanding the size of a swimming pool and the hose used to fill it. This paper proposes a flexible system solution using a three-port converter that optimizes the use of renewable energy and uses the AC power grid (including loads, generators, and renewable energy sources such as wind or PV) to power level 2 EVs corresponding to the charging capacity of the EV and the appropriate voltage level presented in section 2.

2. The proposed converter circuit principle

As with most power sources, determining the system's output load power requirements is a key consideration when selecting a DC/DC converter. With the electric vehicle load having power demand from 2-35 kW with different electric vehicle charging levels (Dutta et al., 2022). Therefore, the proposed converter uses level 2 charging. The DC/DC converter's output requirements include the output voltage and current supplied by the converter to the electric vehicle. The output voltage may have tolerance specifications depending on environmental conditions, such as the input voltage being a renewable energy source or/and from an AC microgrid and the output load current being specifically the EV battery. The load current requirement specifications should include the minimum, maximum, and typical values.

With the above requirements, it is proposed to design an isolated converter that is built with electrically isolated input and output circuits, with no DC path between the input and output. These converters are often used to separate the input and output circuits to avoid electrical noise or dangerous voltage isolation. The circuit diagram has a simple internal structure and is derived from a basic fly-back DC/DC converter and an H-bridge DC/AC converter. The transformer used in the converter works at a high voltage and frequency with a value of 400-1000V/20kHz. The coil connected to the AC microgrid can transfer bidirectional energy. Figure 2 shows the schematic of the converter power circuit, which uses 8 main switches and 3 main switching diodes. In the power converter circuit used when converting energy from PV power source to AC microgrid and battery of electric vehicle by synthesizing Fly-back converter circuit principle, H-bridge, single-phase semi-controlled rectifier bridge. Corresponding to the energy converted from the AC microgrid source to the EV by synthesizing the AC/DC/DC boosting conversion process, this represents a flexible boosting process suitable for the EV charging source.

The working principle of the converter is as follows according to the priority scenarios in order of the scenarios that can operate for the components in the power grid, loads, and distributed energy sources.

Scenario 1 (SC1) is shown in Figure 3 (a): The energy source from the solar battery charges the battery in the electric vehicle with the requirement of fast charging or slow charging as requested by the vehicle owner. The converter functions as a fly-back DC/DC booster. The voltage is increased depending on the transformer ratio between the L1 and L2 coils (transformation ratio m1), the pulse width, and the switching frequency of the switch S1. Described and calculated as expression (1), (2), (3).

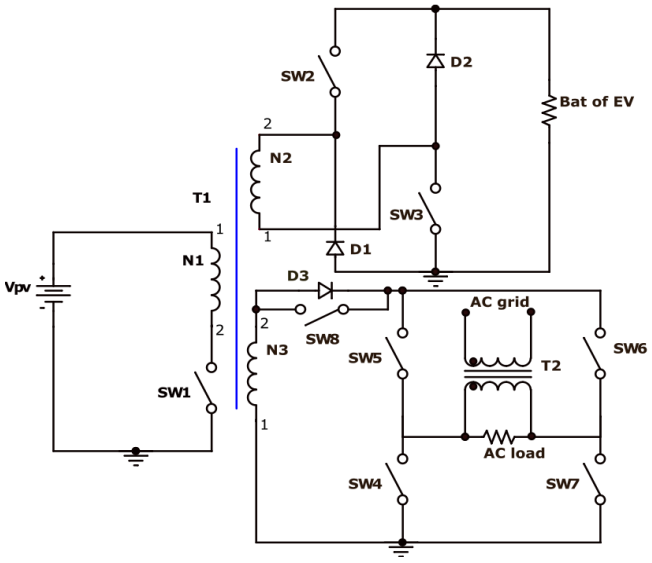

Figure 2 Schematic diagram of the proposed converter

$$V_{DS-SW1} = V_{PV} + V_{batEV}\frac{N_1}{N_2}\,[\mathrm{V}] \tag{1}$$

While the valve is closed, the voltage across the semiconductor valve is zero (ideal). However, when the valve is open, the output voltage is fed back to the primary side of the transformer, and the voltage across the semiconductor switch is increased according to expression (1).

$$V_{batEV} = V_{PV}\frac{N_2}{N_1}\frac{t_1}{T-t_1}\,[\mathrm{V}] \tag{2}$$

$$d1 = \frac{V_{batEV} + V_D}{\frac{V_{PV}}{n_1} + V_{batEV} + V_D} \tag{3}$$

where

T: switching cycle;

t_1 opening time of the SW1 switch is the time interval equal to the SW1 time leads current Corresponding to duty cycle d1

d1: ~~SW1~~ duty cycle of SW1, d1=t_1/T;

N1: number of inductor turns L1;

N2: number of inductor turns L2;

n_1: transformer ratio N1/N2 between the PV source and the electric vehicle;

V_D: Total voltage of switches D1, D2, SW2, and SW3 when conducting current according to two half-cycles of the opening and closing time of switch SW1, as shown in expressions (4) and (5).

$$V_D = d1\,(V_{SW2} + V_{SW3})\,[\mathrm{V}] \tag{4}$$

$$V_D = (1 - d1)(V_{D1} + V_{D2})\,[\mathrm{V}] \tag{5}$$

Figure 3 (a) shows the operating principle of SC1. In this scenario, switches SW1, SW2, and SW3 are active, that is, an incoming control pulse is present. Diodes D1 and D2 are active. The frequency and pulse width are selected as expressions (1), (2), (3).

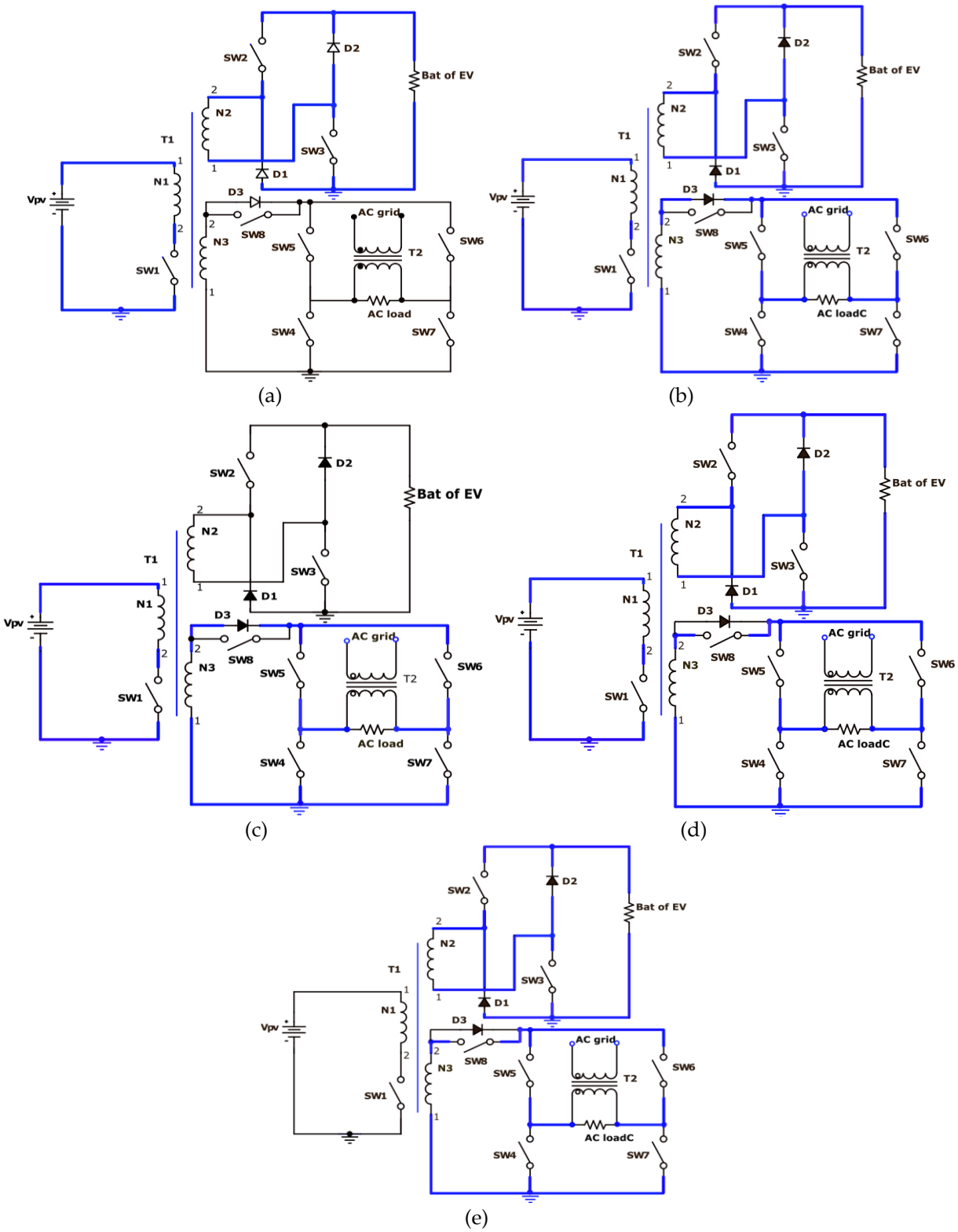

Figure 3 Converter operation: (a) SC1, grid-independent working mode; (b) SC2, grid-connected working mode; (c) SC3, grid-connected working mode; (d) SC4, grid-connected working mode; (e) SC5, grid-connected working mode

Scenario 2 (SC2): The solar energy source charges the battery in the electric vehicle with the requirement of fast or slow charging as requested by the vehicle owner. The converter functions as a fly-back DC/DC booster. The energy is transferred to the grid when the charging energy for the EV decreases. The input voltage for the grid-connected H-bridge circuit is 220 V, which works as a DC/AC unit. The voltage is increased depending on the transformer ratio between coils L1 and L2 (transformer ratio n_1), L1 and L3 (transformer ratio n_2) and the pulse width, and the switching frequency of the switch SW1. Calculated as expression (6), (8), and (9).

The minimum number of primary turns of a pulse transformer that can create the maximum magnetic flux oscillation is determined as expression (6).

$$N1 = \frac{\Delta I_{max} L1}{\Delta B_{max} A_e} 10^{-2} \text{ [turn]} \quad (6)$$

A_e: is the cross-section of the ferrite core, and

ΔI_{max}: Maximum current ripple occurs at the maximum input voltage and minimum duty cycle;

ΔB_{max}: is the maximum allowable magnetic flux depending on the magnetic core type with characteristics according to PO-type ferrite core, calculated according to expression (7):

$$\Delta B_{max} = B_{max} \frac{\Delta I_{pp}}{1.1 * I_{peak}} \text{ [Tesla]} \quad (7)$$

B_{max}: is the maximum allowable magnetic flux density in the magnetic core's operating region;

ΔI_{pp}: Maximum ripple current, $I_{peak} - I_{min}$;

I_{peak}: Maximum ripple current through coil *N1*;

I_{min}: Ripple current minimum through the coil *N1*.

$$\frac{1}{n_2} = \frac{N3}{N1} = \frac{V_{L3} + V_{D3}}{V_{L1}} \quad (8)$$

n_2 transformer ratio between the PV source and the AC microgrid

$$N2 = \frac{V_{L2} + V_{D1}}{V_{L3} + V_{D3}} N3 \text{ [turn]} \quad (9)$$

From expressions (6), (8), and (9), the coil values of *N2*, *N3* of the transformer corresponding to the EV charging input voltage requirement from 400-1000 VDC can be calculated.

Figure 3 (b) shows the specific operation of each switch. In this scenario, the SW8 switch is inactive, SW1-SW7 switches are active, and the diodes D1, D2, and D3 are active. This scenario wastes power on the keys with almost the largest number, so this scenario will be limited in the operating time of this converter. In practice, scenario 2 is operated during the daytime when PV energy is produced from the energy for charging the EV battery. In this scenario, the energy is divided into variable values according to the AC load and EV load requirements. The output voltage for the EV charging station ports and the AC microgrid is determined as expressions (10) and (11).

$$V_{N2} = n_1 V_{PV} . \frac{d1}{1 - d1} \text{ [V]} \quad (10)$$

In which: V_{N2} is the voltage on coil N2 when energy is supplied from the PV source to the EV charging station.

$$V_{N3} = n_2 V_{PV} \frac{d1}{1 - d1} \text{ [V]} \quad (11)$$

In which: V_{N3} is the voltage on coil N3 when energy is supplied from the PV source to the AC microgrid, and the transformer turns ratio for the two PV power source ports and the AC microgrid port.

The output voltage of the two ports in scenario 2 has different values because the value of n_1 and n_2 is different according to the input set and required output of each port. As the EV charging station port is large with an output of up to 1000 VDC, the value of n_1 must be required to be larger than n_2 because the required voltage at the AC microgrid input is in the range of 220-300VDC.

Figure 3(c) shows the PV energy scenario for the AC microgrid load. In scenario 3 (SC3), switches SW1, SW4-SW7 are active and D3 is conducting. The transformer operates at the L3/L1 ratio.

Switches SW2 and SW3 are inactive, and the current through coil L2 is zero. The input voltage value of the H-bridge converter is as shown in Eq. (11).

The energy scenario 4 (SC4) of the battery is charged by two energy sources: PV and AC grid. The converter basically functions as two fly-back units, and the transformer functions as two primary coils L1 and L3. Figure 3 (d) illustrates the operation of the elements in the converter circuit with the SW1-SW8 switches operating, with D3 reverse biased. The conversion process of this scenario converter is performed according to the phase shift time from the L1 and L3 coils to ensure the highest efficiency. By controlling the intermediate circuit between two switches SW1 and SW8, and how to calculate the turns ratio according to the fixed transformer coefficient n_1 and $n_3 = {N2}/{N3}$, the number of turns of the L1 and L3 coils as calculated according to the voltage output for the car load, and the voltage range from 400V-1000V, the PV input voltage from 75V-150V has a voltage gain Gv1, and the voltage from the AC microgrid is 200V-210V has a voltage gain Gv2. Therefore, the voltage gain Gv1 will be from 3.3to8.3; Gv2 will be adjusted from 2 to 5. This issue is proposed by the converter to design so that the control of this scenario is not complicated, and the switches are controlled independently with different parameters.

Scenario 5 (SC5): The charging system for EVs functions as an AC/DC converter with a transformer ratio of m3 (L3 and L2). Solar energy does not work because the weather does not provide favorable operating conditions to produce electricity, affecting the life of the PV system. Figure 3 (e) describes the operation of the elements in the working circuit, such as switches SW2-SW8, Diode D1, D2. The working principle of the converter is performed in 3 specific stages: (1) converting energy from AC/DC through the H-bridge, energy from distributed sources of the AC microgrid, and (2) performing energy conversion to increase voltage by the fly-back principle through the transformer L3 (primary winding) L1 (secondary winding). In this scenario, the voltage gain is Gv2, as in scenario 3 in the operation of the converter. The voltage value is calculated according to the expression (12).

$$V_{N2} = n_3(V_{N3} - V_{SW8})\frac{d2}{1-d2}\,[\mathrm{V}] \tag{12}$$

$$V_{N3} = \frac{2}{\pi}V_{peak}\,[\mathrm{V}] \tag{13}$$

$$V_{peak} = \sqrt{2}.V_{rms}\,[\mathrm{V}] \tag{14}$$

In which: v_{peak} is the peak value of the phase input voltages v_{AC} is the single-phase AC source voltage ($v_{AC} = \sqrt{2}.220.sin\omega t\ (V)$)

V_{rms} is microgrid AC voltage rms value

$d2$ is the duty cycle of SW8

n_3 the turns ratio between the two AC microgrid ports and the EV charging station.

In the case of fast charging, the energy source will focus its capacity on charging loads from renewable energy sources to ensure capacity, current, and charging voltage. In the case of EV charging in the medium level 2 mode, the charging time is from 3-8 hours, the renewable energy source distributes additional energy to the grid and other loads in the charging station system, such as lighting and cooling. The proposed converter analyzed the above scenarios to demonstrate a flexible operation when the charging station uses multiple energy sources at the same time with voltage levels to the charging station varying from 400-1000VDC or uses either energy from the AC microgrid or renewable energy PV. In addition, the renewable PV energy can supply the AC microgrid loads when the charging station has no charging demand.

3. Results of the proposed converter

3.1. Simulation results

The multi-inverter is presented with the working principle in the above section, specifically with 4 scenarios, the simulated input parameters for the converter: Inductance L1=1mH; L2=10mH; L3=1mH; V_{PV}=(75-150)VDC; V_{AC}=220V; V_{Bat-EV}=400-1000VDC. The simulation shows that the value with the specified load value voltage of the EV is 1000 VDC. The implementation process and

simulation results were performed on the principal circuit using Capture AD, and the circuit parameters were measured using PSpice in Orcad software.

SC1: In this scenario, the converter has two energy exchange ports in the direction of the renewable energy source (PV) to the EV charging station. The output voltage at the battery EV has a maximum value of 1000 VDC, the maximum charging capacity is 10 kW, the charging mode is at an average level, and the voltage on SW1 is nearly 610 V. This parameter is used to select the main switches SW1 and SW8. The current through the L1 coil (green line) and the current through SW1 (this main switch is closed) when a control pulse is present. During a pulse, the voltage on SW1 decreases to zero, as shown in the green graph at the measuring point V (SW1: d). The simulation results show that the time when the current appears through SW1 and the voltage on it decreases to zero is a very short time, leading to the damage on this switch being limited to the basic power circuit such as the fly-back set. Power is determined by measuring the PV source and the charging load of the electric vehicle, as shown in Figure 4 (a).

Figure 4(b) shows that the SC2 converters perform energy transfer with three different ports. The energy from the PV source is divided into two parts for the EV charging load and the AC grid load. Power is still prioritized for the EV load with a guaranteed capacity value sufficient for level 2 charging in the range of 2-10kW. The circuit parameters on L2 have been changed to reduce the current value because the capacity at EV is nearly 7.5 kW smaller than that in scenario 1, and the power is partially supplied to the load at the AC grid. The transformer in the converter circuit operates with one primary coil (L1) and two secondary coils (L2 and L3). Similarly, the power is determined by the AVG(-W(Vpv)), AVG(W(Bat)), and AVG(W(AC load)) probes for the DC and AC loads in the system. Figure 4 (b) shows the current voltage on the AC grid load in the form of a signal responding to the AC supply grid.

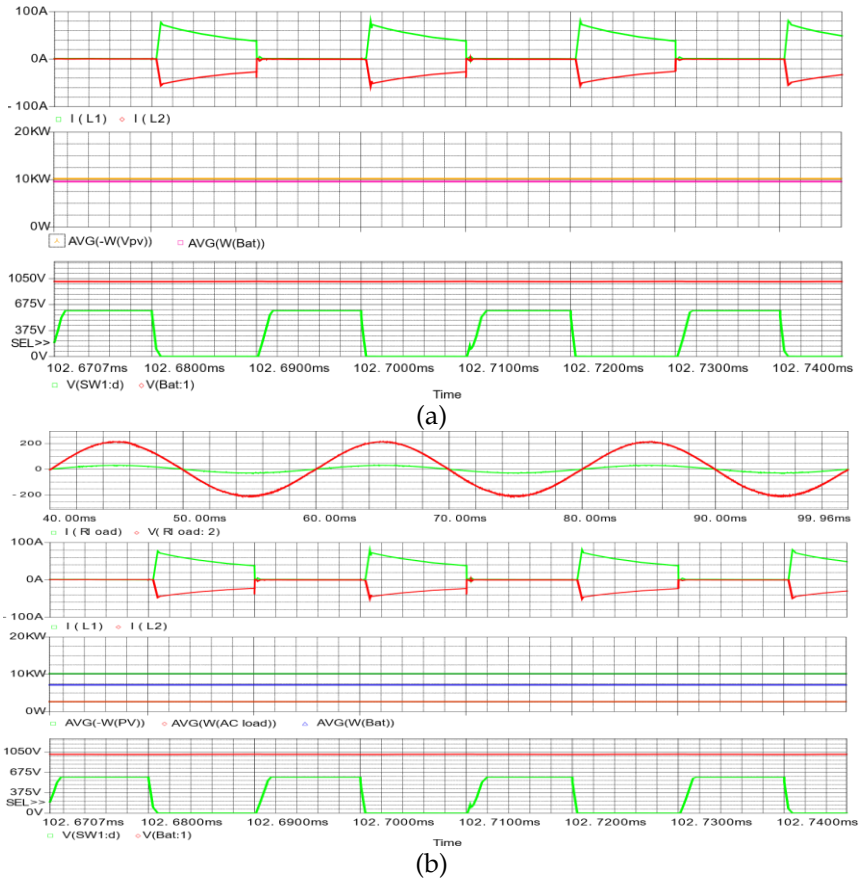

Figure 4 Current, voltage, and power graphs (a) SC1, duty cycle 50%, fsw = 20 kHz; (b) SC2 graph, current, voltage, power, AC load current, and voltage; (c) SC3 graph, current, voltage, power, AC load current, and voltage; (d) SC4 and SC5 graphs, current, voltage, power graph, AC grid current, and voltage

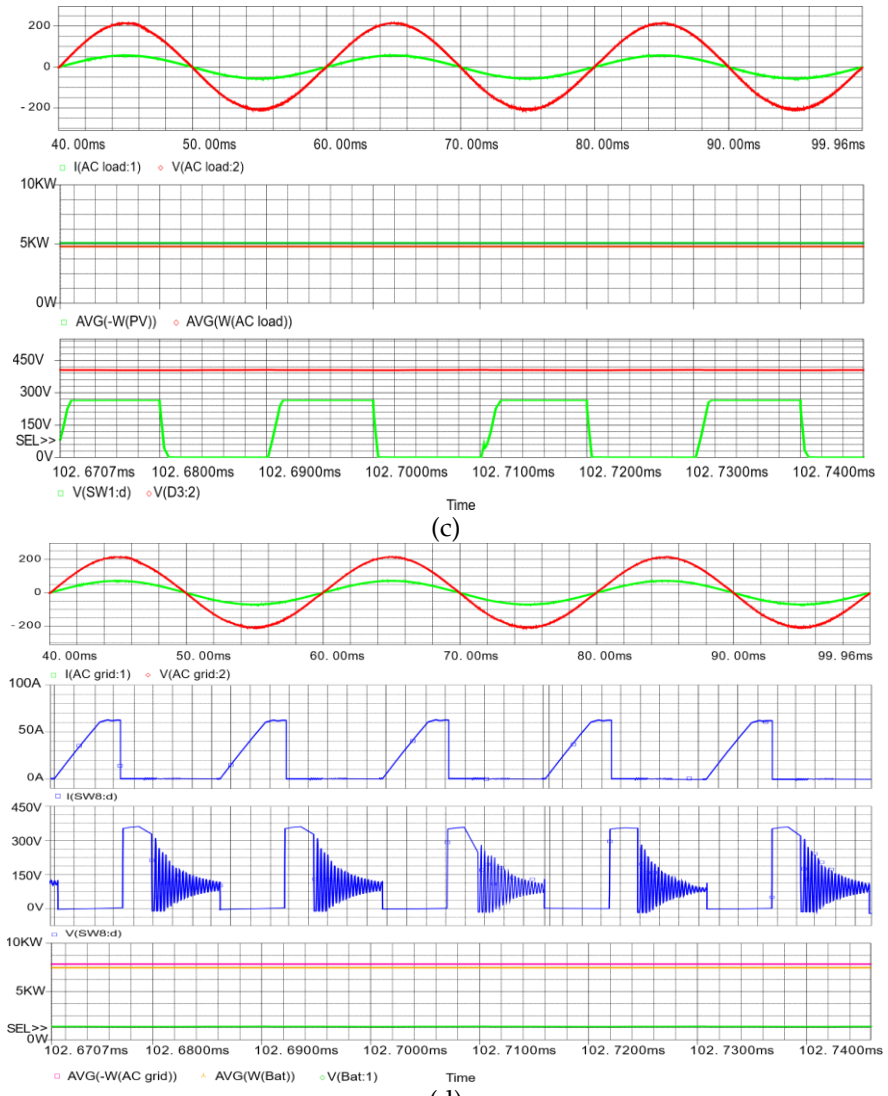

Figure 4 Current, voltage, and power graphs (a) SC1, duty cycle 50%, fsw = 20 kHz; (b) SC2 graph, current, voltage, power, AC load current, and voltage; (c) SC3 graph, current, voltage, power, AC load current, and voltage; (d) SC4 and SC5 graphs, current, voltage, power graph, AC grid current, and voltage (Cont.)

The SC3 simulation is shown in Figure 4(c). The voltage on switch SW1 and the DC/AC converter input voltage are close to 400 VDC. The conversion power is 5 kW. When the EV load is not consumed, the PV energy is fully supplied to the AC microgrid load. The sensors still show the values of the SW1 element, the PV input power, and the AC load output power.

SC4 and SC5 simulations are shown in Figure 4 (d). Scenario 4: PV energy and AC microgrid power are supplied to the EV, which performs the same operating principle as scenario 1. Therefore, the simulation will perform different values from case 1 with some probes as in SW8. The voltage on SW8 is nearly 365 V at probe V(SW8:d) smaller than the voltage on SW1 in Scenarios 1, 2, and 3. Therefore, selecting the switch SW8 using scenario 1 is possible. The current and voltage at the SW8 are almost zero, leading to a small loss in the SW8 operation at probes V(SW8:d) and I(SW8:d). The output voltage for charging the electric car is 1000 VDC at the V(bat) measuring pin. Figure 4 (d) shows the current and voltage on the AC supply grid. The measured power in Scenarios 4 and 5 is shown by the AVG(-W(AC grid)) and AVG(W(Bat) measuring heads). The voltage required for the charging load is 1000 VDC, ensuring the required value.

When performing simulations in the scenarios, the input values are adjusted to fluctuate within the maximum power range of 10 kW. The simulation results corresponding to the scenarios describing the current, voltage, and power values on the elements in the converter circuit are given to perform parameter selection for the components for safe and optimal experimentation.

Figure 5 (a) shows the calculated simulation results corresponding to the efficiency of the power exchange between the three ports: (1) PV energy source, (2) AC grid supply, and (3) electric carload with charging voltage of 400 VDC and output power. Figure 5 (a) shows the efficiency of the scenarios with higher efficiency than the values of the converter (Al Sakka et al., 2011). The average value of the converter efficiency is 95.4%. SC1 has an average efficiency of 95.7%, scenarios 3, 4, and 5 have an average efficiency of more than 95.0%, and scenario 2 has the highest average efficiency of 96.0%.

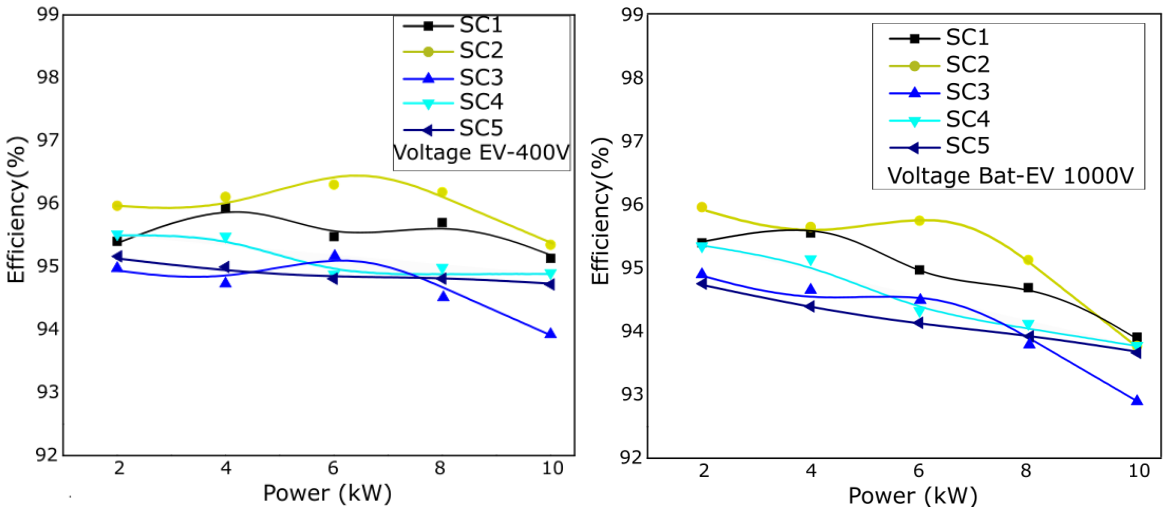

Figure 5 Computed performance for the scenarios in the proposed converter: (a) 400 VDC voltage and (b) 1000 VDC output voltage

Figure 5 (b) shows specific scenarios corresponding to the input voltage of charging the electric vehicle at 1000 VDC and output power, at which the parameters, such as voltage gain and pulse width of the SW1 and SW8 switches, are changed. The switching frequency is 20 kHz. Figure 5 (b) shows that the efficiency of the scenarios is higher than the values of the converter (Al Sakka et al., 2011). The highest efficiency in scenario 2 at 2 kW capacity is 96.0%, and the lowest efficiency of the converter is SC3 corresponding to 10 kW capacity with 93.0%. In this case, the charging voltage of 1000 VDC leads to a decrease in the converter's efficiency because the duty cycle of the main switches SW1 and SW8 needs to be increased.

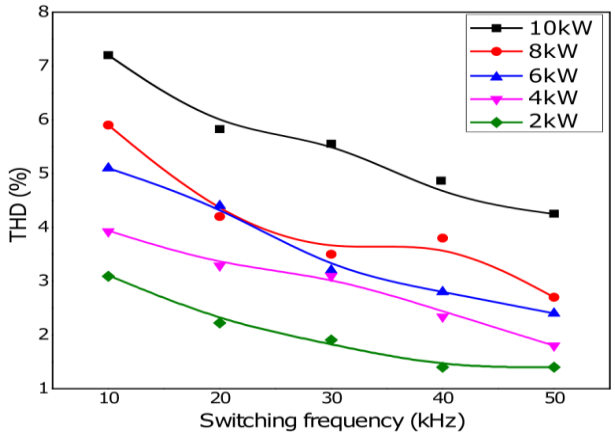

Figure 6 TDH case of AC/DC conversion, switching frequency from 10 to 50 kHz

Figure 6 illustrates the influence of the switching frequency for switches SW1 and SW8 on the harmonic distortion of the output voltage of the converter corresponding to SC4 and SC5. The simulated power ranges from 2-10kW. The simulation results show that with a high-power value of 10 kW, the total harmonic value is large, and with a large switching frequency, the total harmonic TDH (%) decreases from 7.2% to 4.7%, corresponding to a frequency increase of 10kHz-50kHz. The smallest total harmonic value corresponding to a 2 kW switching power from the grid to the EV charging station is less than 3%. With 5 kW power, the total harmonic TDH (%) of the converter is below 4.5%.

3.2. Experimental description of the converter

Figure 7 shows the experimental image of the proposed system and converter with the input parameters listed in Table 1. The PV energy source is represented by a DC source with a variable power input from 2-10 kW with the corresponding current and voltage of the source. In this study, the power of the PV source is the maximum power point. The AC microgrid has loads and sources from the distribution grid.

Table 1 shows the experimental input parameters for the multi-port converter to efficiently perform flexible operation functions using energy from PV sources. In which the parameters are implemented with actual power used to charge EVs and supply loads in the AC microgrid.

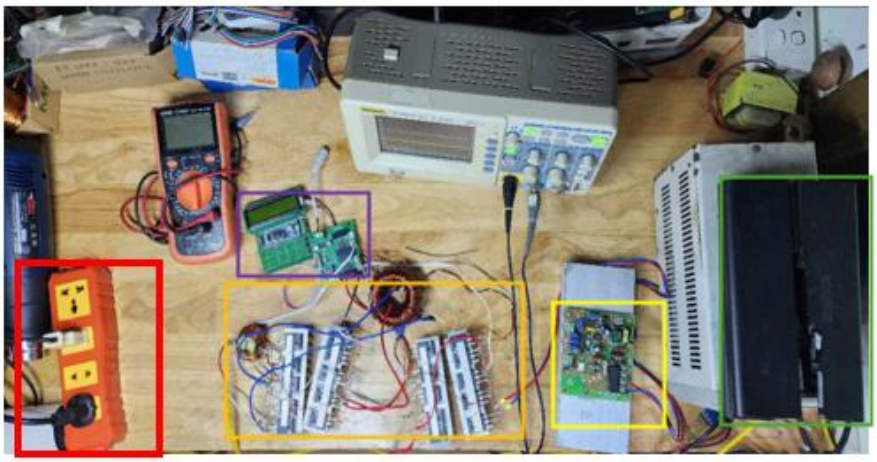

Figure 7 Experimental image of the converter. The yellow frame represents the PV energy source, the orange frame represents the converter, the green frame represents the EV battery, the red frame represents the AC microgrid, and the purple frame represents the controller

Table 1 Experimental parameters of the converter

Experimental Equipment	Parameters
PV output voltage	75-150VDC
PV power	7kW
EV charging voltage	400-1000VDC
EV charging power	2-10kW
AC microgrid	220V, 50Hz, 2-10kW
Pulse transformer T1	L1, L3:1mH; L2: 10mH
Transformer T2	220V, 50Hz, 6kW
SW1 switch	GW80H65DFB
SW2-SW8 switchs	GT30J127
Diodes D1-D3	MURP20040CT
AC microgrid load	2-6kW
PV output filter capacitor, EV charging input, H-bridge input	10μF, 47μF
Electric vehicle battery	Lithium, 3kW

The experimental implementation results of the converter for each specific case with current, voltage, and power corresponding to different actual values of ports such as EV, AC microgrid load, and PV source fluctuations, are given in the Supplementary Materials.

Figure 8 (a) compares the experimental and simulation results for each operating case of the converter in the system. SC1 voltage value of 400 VDC at EV load, the actual energy loss on the larger power switches leads to a smaller actual efficiency with an average value of nearly 1% in scenario 1. With the corresponding EV input voltage of 1000 VDC, the actual efficiency is nearly 1.2% smaller, as shown in Figure 8 (b). Thus, the energy conversion process depends on the input and output voltage parameters, the main switch control process of the converter. Figures 8 (a) and (b) are similar to SC2, SC3, SC4, and SC5, corresponding to the largest experimental circuit error value of 1.3%. The SC1 and SC5 converters have higher efficiency than SC2, SC3, and SC4 because the number of working switches is less. At 1000VDC EV input voltage of 1000 VDC, the experimental average efficiency is less than the EV input voltage value of 400 VDC. The energy is controlled to implement scenarios of efficient use and optimal requirements for renewable energy sources, as in SC1, SC2, SC3, and SC4. In the case of SC5, the EV charging station energy will use energy from the AC microgrid. The system will control the use of energy from renewable energy sources when there is surplus according to the load path of the AC microgrid. In this case, when the PV energy source is not active in the evening, EV owners are also encouraged to limit charging at peak times and do it after the peak load time around 9 PM.

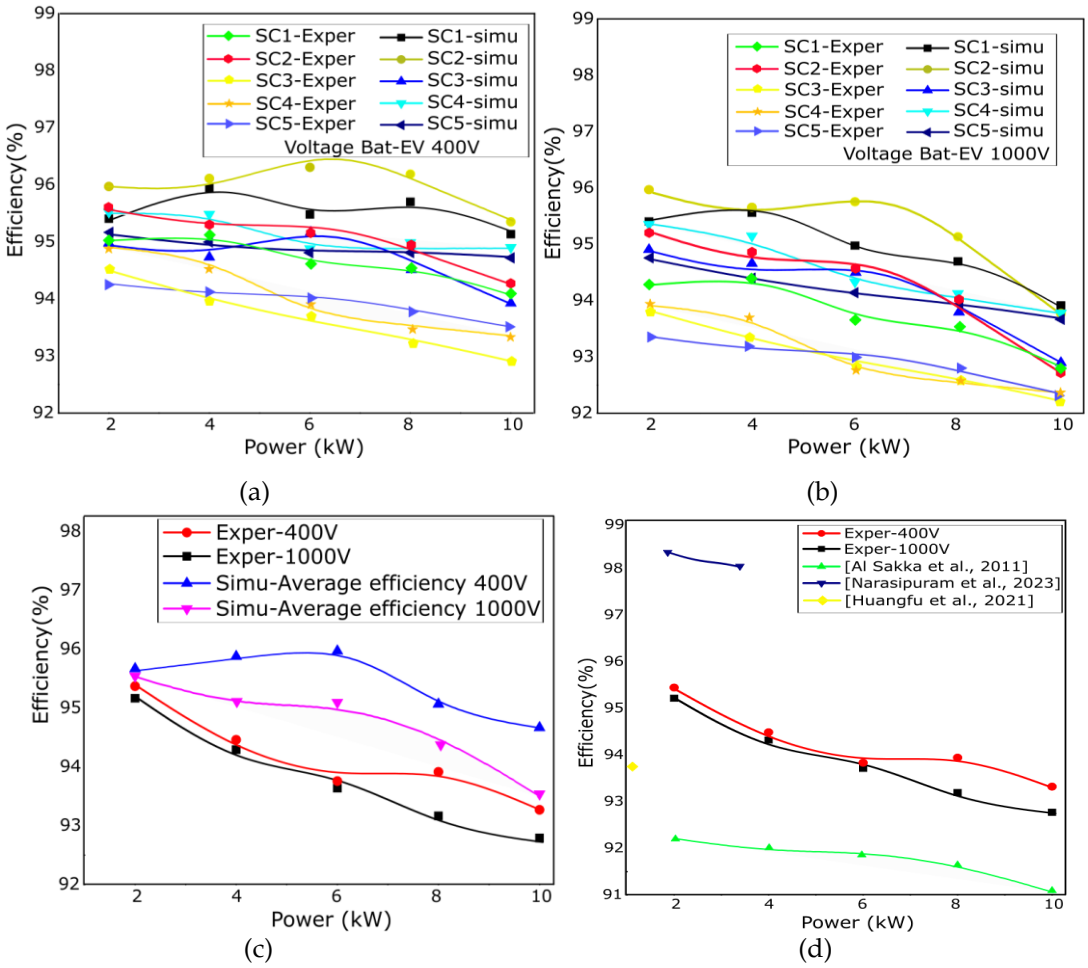

Figure 8 Experimental performance comparison: (a) experimental performance comparison with simulation in case of EV charging voltage of 400 VDC; (b) experimental performance comparison with simulation in case of EV charging voltage of 1000 VDC; (c) average experimental performance comparison with simulation of the proposed converter; (d) comparison of the proposed converter with the reference

In this study, the operational response for the EV charging station load and the load from the actual AC microgrid are presented. SC1, SC2, and SC3 show full use of separate independent renewable energy sources connected to the proposed converter. Scenario 4 shows that renewable energy tends to decrease in capacity, leading to the need to use other renewable energy sources from the AC microgrid to supply the EV charging station.

Figure 8 (c) shows the average conversion efficiency of the converter performing 5 experimental scenarios corresponding to the EV charging voltage, compared with the simulation results of the proposed converter. The converter efficiency with the highest average value of 96% corresponds to the simulation results' 6kW, 400VDC capacity. The smallest efficiency of 92.7% corresponds to the 10 kW, 1000 VDC capacity of the experimental results. Thus, the experimental implementation has an error of about 2% between the simulation and experimental results corresponding to the EV charging voltage of 1000 VDC. The error with the EV charging voltage value of 400 VDC is approximately 1%. From the experimental results of the converter, we can see that the efficiency value of the converter is high compared to the reference results when this proposed converter has to perform many different functions between the ports from the AC microgrid and the PV renewable energy source with the goal of providing power to the flexible EV charging station with many different scenarios of the system performing energy conversion with different types of DC/DC or DC/AC or AC/DC or both DC/DC and DC/AC. The study with the charging voltage value for EVs in this case demonstrates the feasibility of developing a power-boosting charging converter to serve level 3 fast charging for EVs. With the charging input voltage for EVs adjustable from 400-1000VDC, it is possible to apply to level 3 fast chargers, increasing the operating range by increasing the higher voltage, EVs can achieve a larger operating range in a shorter charging time. Moreover, with the voltage value of 1000 VDC, the efficiency of the proposed converter is quite high, and it is possible to increase the charging capacity for EVs by connecting the proposed converters in parallel with independent ports such as PV source, AC microgrid, and EV charging station.

Figure 8(d) compares the experimental results of the proposed flexible converter with those of previous studies (Narasipuram and Mopidevi, 2023; Huangfu et al., 2021; Al Sakka et al., 2011). Al Sakka et al. (2011) showed a simulated power value of up to 30 kW with a DC/DC converter with an efficiency of up to 92% when boosting in the power range corresponding to the proposed 10kW converter, (Al Sakka et al., 2011) achieved nearly 87%. Narasipuram and Mopidevi (2023) simulated a small capacity DC/DC converter of 3.5 kW with an efficiency of over 98%. The paper (Huangfu et al., 2021) performed with a small capacity of 200 W with an efficiency of 92.3%. The results show that the experimental converter corresponding to the initial power output for level 2 EV charging has an efficiency value in the range of about 2.5% higher than the converter and lower than the level 1 EV charging value.

4. Conclusions

This study provides research on flexible operations that can optimally use distributed energy in an AC microgrid and distributed PV source connected directly to EV charging stations. The power circuit is isolated from the gate section. Capable of providing multiple output voltages, all isolated from the AC microgid and PV sources. Adjust multiple output voltages from 400-1000 VDC with a single controller. It can operate on various input voltages according to the variation of renewable energy sources 75-150 VDC and has a higher value at a voltage of 220 VDC from the AC microgrid. The proposed converter uses a few components to simplify the control of the system and integrate the distribution grid with the load at multiple ports. The average experimental efficiency of the largest converter is more than 95%, which is a feasibility study result contributing to the energy conversion process in renewable energy sources connected to the grid. In addition, the maximum experimental power of 10 kW is capable of charging EVs to level 2, but with this converter, the power can be increased to level 3 charging without changing the converter structure. The number of converters in parallel with the charging port and AC microgrid is only needed. Total harmonics below 7.2% of the converter are within the allowable power conversion range, ensuring power

quality for the port load. Electric vehicle charging stations using solar energy have a positive impact on both the electric vehicle and energy industries. The development of charging stations contributes to promoting the demand for EVs. Both forms significantly contribute to environmental protection and cost savings. Flexible charging station systems using PV rooftops located on AC microgrids and at charging stations not only serve the purpose of charging vehicles but also provide utilities while waiting for EVs to charge and the load on the supply grid. This converter contributes to the plan to build a network of solar-powered electric vehicle charging station infrastructure in Vietnam with the operation of different flexible scenarios.

Acknowledgements

The research team would like to thank the Posts and Telecommunications Institute of Technology Hanoi, Vietnam for creating favorable conditions during the implementation of the research content of this article.

Author Contributions

Nguyen The Vinh: Conceptualization, formal analysis, data validation, writing – review & editing, visualization, supervision, Writing – original draft, software, experiment, data collection, data analysis & interpretation. Nguyen Van Dung: Conceptualization, literature review, methodology, investigation, writing – original draft, writing – review & editing. All authors have read and agreed to the published version of the manuscript.

Conflict of Interest

The authors declare no conflict of interest.

References

Ahmad, F & Bilal, M 2023, 'A comprehensive analysis of electric vehicle charging infrastructure, standards, policies, aggregators and challenges for the Indian market', *Energy Sources, Part A: Recovery, Utilization, and Environmental Effects*, vol. 45, no. 3, pp. 8601–8622, https://doi.org/10.1080/15567036.2023.2228734

Ajiwiguna, TA & Kirom, MR 2024, 'Uninterrupted electricity supply using off-grid solar PV systems for remote areas', *International Journal of Technology*, vol. 15, no. 5, pp. 1561–1572, https://doi.org/10.14716/ijtech.v15i5.6089

Al Sakka, M, Van Mierlo, J & Gualous, H 2011, 'DC/DC converters for electric vehicles', In: *Electric vehicles—Modelling and simulation*, chapter 13, pp. 310–330, https://doi.org/10.5772/17048

Al-Ogaili, AS, Aris, I, Sabry, AH, Othman, ML, Azis, N, Isa, D & Hoon, Y 2017, 'Design and development of three-levels universal electric-vehicle charger based on integration of VOC and SPWM techniques', *Journal of Computational and Theoretical Nanoscience*, vol. 14, pp. 4674–4685, https://doi.org/10.1166/jctn.2017.6881

Aravindan, KL, Izzat, MA, Ramayah, T, Chen, TS, Choong, YV, Annamalah, S, Ilhavenil, N & Ahmad, AB 2023, 'Determinants of electric car patronage intention', *International Journal of Technology*, vol. 14, no. 6, pp. 1393–1401, https://doi.org/10.14716/ijtech.v14i6.6624

Balagopal, B, Huang, CS & Chow, M 2017, 'Effect of calendar aging on Li-ion battery degradation and SOH', *In:* 43rd Annual Conference of the IEEE Industrial Electronics Society (IECON 2017), pp. 7647–7652, https://doi.org/10.1109/IECON.2017.8217340

Bradley, TH & Frank, AA 2009, 'Design, demonstrations and sustainability impact assessments for plug-in hybrid electric vehicles', *Renewable and Sustainable Energy Reviews*, vol. 13, no. 1, pp. 115–128, https://doi.org/10.1016/j.rser.2007.05.003

Bukhariv, SMAS, Maqsood, J, Baig, MQ, Ashraf, S & Khan, TA 2015, 'Comparison of characteristics—lead acid, nickel based, lead crystal and lithium based batteries', *In:* 2015 17th UKSim-AMSS International Conference on Modelling and Simulation (UKSim), Cambridge, UK, pp. 444–450, https://doi.org/10.1109/UKSim.2015.69

Busch, P, Pares, F, Chandra, M, Kendall, A & Tal, G 2024, 'Future of global electric vehicle supply chain: Exploring the impact of global trade on electric vehicle production and battery requirements', *Transportation Research Record*, vol. 2678, no. 11, pp. 1468-1482, https://doi.org/10.1177/03611981241244797

Chakraborty, S, Vu, H-N, Hasan, MM, Tran, D-D, Baghdadi, ME & Hegazy, O 2019, 'DC-DC converter topologies for electric vehicles, plug-in hybrid electric vehicles and fast charging stations: State of the art and future trends', *Energies*, vol. 12, no. 8, article 1569, https://doi.org/10.3390/en12081569

Dutta, B, Jaiswal, S, Phatarpekar, V, Tayal, VK & Singh, HP 2022, 'Design and implementation of a 3-level battery management system (BMS) for an electric vehicle', *In:* SK Natarajan, R Prakash & K Sankaranarayanasamy (eds), *Recent advances in manufacturing, automation, design and energy technologies*, Lecture Notes in Mechanical Engineering, Springer, Singapore, https://doi.org/10.1007/978-981-16-4222-7_85

Fontaras, G, Zacharof, NG & Ciuffo, B 2017, 'Fuel consumption and CO_2 emissions from passenger cars in Europe—laboratory versus real-world emissions', *Progress in Energy and Combustion Science*, vol. 60, pp. 97–131, https://doi.org/10.1016/j.pecs.2016.12.004

Government of Vietnam 2018, *Decision No. 519/QĐ-TTg (11 May 2018) approving the investment policy of the project "Application of smart grid to develop renewable energy sources and efficient energy use (SGRE-EE)"*

Government of Vietnam 2022, *Decision No. 876/QĐ-TTg (22 July 2022) approving the action program on green energy conversion, carbon and methane emission reduction of the transport sector*

Hadley, SW & Tsvetkova, AA 2009, 'Potential impacts of plug-in hybrid electric vehicles on regional power generation', *The Electricity Journal*, vol. 22, pp. 56–68, https://doi.org/10.1016/j.tej.2009.10.011

Hegazy, O, Barrero, R, Van Mierlo, J, Lataire, P, Omar, N & Coosemans, T 2013, 'An advanced power electronics interface for electric vehicles applications', *IEEE Transactions on Power Electronics*, vol. 28, pp. 5508–5521, https://doi.org/10.1109/TPEL.2013.2256469

Huangfu, Y, Ma, R, Zhao, B, Liang, Z, Ma, Y, Wang, A, Zhao, D, Li, H & Ma, R 2021, 'A novel robust smooth control of input-parallel output-series quasi-Z-source DC-DC converter for fuel cell electrical vehicle applications', *IEEE Transactions on Industry Applications*, vol. 57, no. 4, pp. 4207–4221, https://doi.org/10.1109/TIA.2021.3073643

Ikeya, T, Sawada, N, Murakami, JI, Kobayashi, K, Hattori, M, Murotani, N, Ujiie, S, Kajiyama, K, Nasu, H, Narisoko, H, Tomaki, Y, Adachi, K, Mita, Y & Ishihara, K 2002, 'Multi-step constant-current charging method for an electric vehicle nickel/metal hydride battery with high energy efficiency and long cycle life', *Journal of Power Sources*, vol. 105, pp. 6-12, https://doi.org/10.1016/S0378-7753(01)00907-7

Islam, MR, Shah, MR & Ali, MH 2021, *Emerging power converters for renewable energy and electric vehicles: Modeling, design, and control*, 1st edn, CRC Press, https://doi.org/10.1201/9781003058472

Jamahori, HF, Abdullah, MP, Ali, A & AlKassem, A 2024, 'Optimal design and performance analysis of multiple photovoltaic with grid-connected commercial load', *International Journal of Technology*, vol. 15, no. 4, pp. 834–846, https://doi.org/10.14716/ijtech.v15i4.6019

Jayakumar, A, Chalmers, A & Lie, TT 2017, 'Review of prospects for adoption of fuel cell electric vehicles in New Zealand', *IET Electrical Systems in Transportation*, vol. 7, pp. 259–266, https://doi.org/10.1049/iet-est.2016.0078

Jones, B, Nguyen-Tien, V & Elliott, RJR 2023, 'The electric vehicle revolution: Critical material supply chains, trade and development', *The World Economy*, vol. 46, no. 1, pp. 2-16, https://doi.org/10.1111/twec.13345

Khan, F, Ali, Y & Khan, AU 2020, 'Sustainable hybrid electric vehicle selection in the context of a developing country', *Air Quality, Atmosphere & Health*, vol. 13, pp. 489–499, https://doi.org/10.1007/s11869-020-00812-y

Kopacz, R, Menzi, D, Krismer, F, Rąbkowski, J, Kolar, JW & Huber, J 2024, 'New single-stage bidirectional three-phase AC-DC solid-state transformer', *Electronics Letters*, vol. 60, no. 2, article e13084, https://doi.org/10.1049/ell2.13084

Linh, NH, Viet, TH, Sørensen, RM, Venturini, G, Petrović, S, Jaenicke, TL & Nielsen, DBV 2024, *Viet Nam energy outlook report: Pathways to net-zero*, EREA & DEA

Liu, K, Li, K, Peng, Q & Zhang, C. 2019, 'A brief review on key technologies in the battery management system of electric vehicles', *Frontiers of Mechanical Engineering*, vol. 14, pp. 47–64, https://doi.org/10.1007/s11465-018-0516-8

Musavi, F, Cracium, M, Gautam, DS & Eberle, W 2014, 'Control strategies for wide output voltage range LLC resonant DC-DC converters in battery chargers', *IEEE Transactions on Vehicular Technology*, vol. 63, no. 3, pp. 1117–1125, https://doi.org/10.1109/TVT.2013.2283158

Narasipuram, RP & Mopidevi, S 2023, 'A novel hybrid control strategy and dynamic performance enhancement of a 3.3 kW GaN-HEMT-based iL2C resonant full-bridge DC-DC power converter methodology

for electric vehicle charging systems', *Energies*, vol. 16, no. 15, article 5811, https://doi.org/10.3390/en16155811

Nurulin, YR, Skvortsova, IV & Konovalova, OA 2023, 'Innovation management models in the energy sector', *International Journal of Technology*, vol. 14, no. 8, pp. 1759–1768, https://doi.org/10.14716/ijtech.v14i8.6846

Onibonoje, MO, Alegbeleye, OO & Ojo, AO 2023, 'Control design and management of a distributed energy resources system', *International Journal of Technology*, vol. 14, no. 2, pp. 236–245, https://doi.org/10.14716/ijtech.v14i2.5884

Rangarajan, S, Sunddararaj, SP, Sudhakar, AV, Shiva, CK, Subramaniam, U, Collins, ER & Senjyu, T 2022, 'Lithium-ion batteries—the crux of electric vehicles with opportunities and challenges', *Clean Technologies*, vol. 4, pp. 908–930, https://doi.org/10.3390/cleantechnol4040056

Spingler, F, Wittmann, W, Sturm, J, Rieger, B & Jossen, A 2018, 'Optimum fast charging of lithium-ion pouch cells based on local volume expansion criteria', *Journal of Power Sources*, vol. 393, pp. 152–160, https://doi.org/10.1016/j.jpowsour.2018.04.095

Thang, PN, Vinh, VT & Vinh, NT 2020, 'A flexible DC-DC converter for the battery-DC bus renewable energy system', *International Energy Journal*, vol. 20, no. 4, pp. 581–594

Thomas, CE 2009, 'Fuel cell and battery electric vehicles compared', *International Journal of Hydrogen Energy*, vol. 34, pp. 6005–6020, https://doi.org/10.1016/j.ijhydene.2009.06.003

Vinh, NT & Dung, NV 2025, 'Bidirectional AC/AC converter linking two microgrids in a flexible microgrid', *International Journal of Power Electronics and Drive System*, vol. 16, no. 1, pp. 389–406, https://doi.org/10.11591/ijpeds.v16.i1.pp389-406

Vinh, NT 2023, 'Bidirectional converter connecting the energy storage system to the DC and AC grid', *International Energy Journal*, vol. 23, no. 3, pp. 141–154

Vinh, VT, Vinh, NT & Dai, LV 2022, 'Partly-isolated DC-DC converter for DC bus battery-PV solar energy system', *GMSARN International Journal*, vol. 16, no. 3, pp. 267–272

Wood, DL, Quass, JD, Li, J, Ahmed, S, Ventola, D & Daniel, C 2018, 'Technical and economic analysis of solvent-based lithium-ion electrode drying with water and NMP', *Drying Technology*, vol. 36, pp. 234–244, https://doi.org/10.1080/07373937.2017.1319855

Yamamoto, O 2014, 'The lithium-air battery: Fundamentals', In: *N Imanishi, AC Luntz & P Bruce* (eds), Springer, New York, https://doi.org/10.1007/978-1-4899-8062-5

Young, K, Wang, C, Wang, LY & Strunz, K 2013, 'Electric vehicle battery technologies', in R García-Valle & JAP Lopes (eds), *Electric vehicle integration into modern power networks*, Springer, New York, chapter 2, https://doi.org/10.1007/978-1-4614-0134-6_2